

Interfacial oxide growth at silicon/high-*k* oxide interfaces: First principles modeling of the Si–HfO₂ interface

M. H. Hakala^{a)} and A. S. Foster

Laboratory of Physics, Helsinki University of Technology, P.O. Box 1100, FIN-02150 HUT, Finland

J. L. Gavartin

Department of Physics and Astronomy, University College London, Gower Street, London WC1E 6BT, United Kingdom

P. Havu, M. J. Puska, and R. M. Nieminen

Laboratory of Physics, Helsinki University of Technology, P.O. Box 1100, FIN-02150 HUT, Finland

(Received 19 December 2005; accepted 29 June 2006; published online 22 August 2006)

We have performed first principles calculations to investigate the structure and electronic properties of several different Si–HfO_x interfaces. The atomic structure has been obtained by growing HfO_x layer by layer on top of the Si(100) surface and repeatedly annealing the structure using *ab initio* molecular dynamics. The interfaces are characterized via their geometric and electronic properties, and also using electron transport calculations implementing a finite element based Green's function method. We find that in all interfaces, oxygen diffuses towards the interface to form a silicon dioxide layer. This results in the formation of dangling Hf bonds in the oxide, which are saturated either by hafnium diffusion or Hf–Si bonds. The generally poor performance of these interfaces suggests that it is important to stabilize the system with respect to lattice oxygen diffusion. © 2006 American Institute of Physics. [DOI: 10.1063/1.2259792]

I. INTRODUCTION

The impressive increase in the performance of micro-electronic devices during the past few decades has been made possible by continuous transistor scaling based on a reduction in the thickness of the gate dielectric in typical metal-oxide-semiconductor field-effect transistors (MOSFETs). At present MOSFET scaling approaches a physical limit, as further reduction leads to a large increase in the leakage current due to direct tunneling across the thin silicon dioxide (SiO₂) layer. Several possible approaches to resolve this are being considered,^{1–3} but retaining conventional MOSFET design remains an economically attractive choice, and a leading option is just to replace SiO₂ with another oxide of higher dielectric constant (high *k*). A high-*k* oxide would provide higher effective capacitance to a comparable SiO₂ layer, hence allowing thicker layers to be used to reduce losses due to tunneling. The specific choice of oxide is determined by a set of requirements⁴ based on both the intrinsic properties of the grown oxide and its integration into the fabrication process, and at present hafnium oxide (HfO₂) remains a leading candidate.

Although progress is being made, high-*k* oxide devices still suffer from several critical performance issues^{5,6} related mainly to the growth of a SiO₂ interfacial layer and generation of defects in HfO₂. The interfacial layer leads to a reduction of the dielectric constant and, hence, the effective capacitance of the interface. Defects at the interface and in the bulk oxide trap charge reduce channel mobility (deep traps), increase leakage current (shallow traps),^{2,7–9} and causing instability of the threshold voltage.¹⁰ In standard

MOSFET fabrication, defects in SiO₂ are passivated by hydrogen, but in HfO₂ this causes as many problems as it solves.¹¹ Various other postdeposition treatments have been tried, especially nitrogen-based,¹² but with little success in reducing fixed charge in the insulator.

General preparation practice has been to fabricate an oxide layer with as thin a SiO₂ interfacial layer as possible, and with a minimal density of defects. Initially, an ideal system was thought to consist of a perfect interface between crystalline silicon and HfO₂, with no defects, providing maximum effective capacitance and minimum effects on channel mobility and leakage. Theoretical approaches to modeling the Si–HfO₂ interface have taken this ideal as a basis, and several models have been generated.^{13–16} However, the experimental consensus seems to indicate that such an interface structure never exists in reality, and the real interface can be characterized as always Si–SiO_x–HfO₂ (for example, see Refs. 17 and 18). In this study we investigate the stability of the ideal Si–HfO₂ interface with respect to deposition of a nonstoichiometric and stoichiometric HfO_x film, and also consider the formation of defects within the film.

II. METHODS

The calculations were performed using the linear combination of atomic orbitals basis SIESTA code,^{19,20} implementing the density functional theory (DFT) within the generalized gradient approximation. We used the functional of Perdew, Burke, and Ernzerhof.²¹ Core electrons are represented by norm-conserving pseudopotentials using the Troullier-Martins parametrization. The pseudopotential for the silicon atom was generated in the electron configuration [Ne]3s²3p², for oxygen in [1s²]2s²2p⁴, for hafnium in

^{a)}Electronic mail: mhh@fyslab.hut.fi

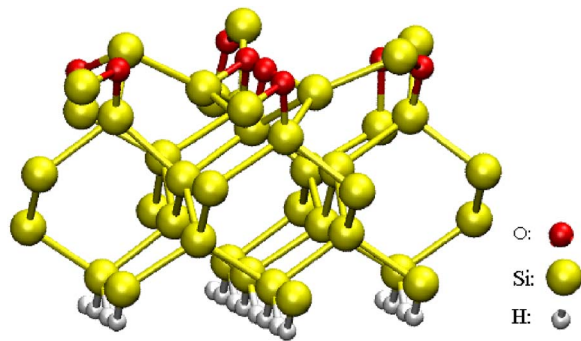


FIG. 1. (Color online) Relaxed structure of the silicon surface after addition of terminating oxygen species.

[Xe, $4f^{14}$] $6s^25d^2$, and for hydrogen in $1s^1$, with the square brackets denoting the core electron configurations. The basis set for the combined system was optimized to provide high accuracy and flexibility. The system's properties were converged with respect to k points ($2 \times 2 \times 1$ mesh) and mesh (corresponding to an energy cutoff of 150 Ry). Initial calculations on silicon, silicon dioxide, and the different bulk phases of hafnia using this setup showed good agreement with experiment. Note that the general underestimation of band gaps in DFT means that absolute values in the calculated band structure have a large error margin. Various, somewhat empirical, methods can be used to correct for this problem,^{16,22} but here we focus on the trends and total-energy differences between systems.

In addition, electron transport properties were calculated using the Green's function method within the framework of the DFT,²³ with a finite element implementation.^{24,25} This models ballistic tunneling between two leads, and includes both direct and resonant tunnelings. The description of the current is analogous to the Landauer-Büttiker model.²⁶ The tunneling probabilities are calculated using four k points.

The initial setup of our modeled structure always consists of a periodic slab with four layers of Si(100) forming the (2×1) reconstruction at the surface, with the bottom layer terminated by hydrogen (see Fig. 1). The lowest layer silicons and hydrogens were kept frozen during simulations, while all other atoms were relaxed until forces were less than 0.02 eV/\AA . Following previous studies of silicon-hafnia interface growth,¹⁵ all the silicon dangling bonds on the upper silicon surface were terminated by oxygens (see Fig. 1). Our interfaces were then *grown* by cycles of hafnia layer deposition, simulated annealing, and high accuracy relaxation (similar to the method used in Ref. 27). After depositing a layer of hafnia the whole system is relaxed to the ground state, and we then perform a molecular dynamics simulation using a Nosé thermostat at a temperature of 600 K and a timestep of 5 fs. Once the run is equilibrated, we anneal down to 0 K, and perform a final relaxation. Then the next layer of hafnia is added. This method provides a much better sampling of the energy landscape of possible structures than is possible from static relaxation alone.

To model a nonstoichiometric interface we deposited three layers of cubic HfO (with a slightly expanded lattice constant to match the silicon surface) onto the surface, providing a final atomic supercell configuration of $\text{Hf}_{24}\text{O}_{32}$ on

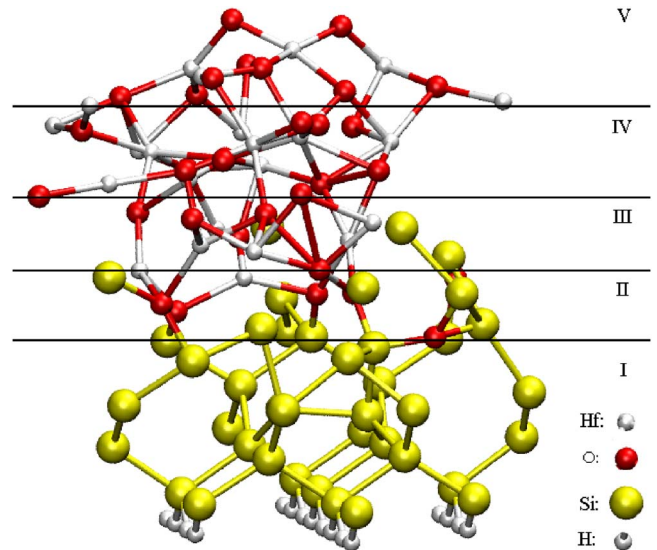


FIG. 2. (Color online) Relaxed structure of the nonstoichiometric Si-HfO₂ interface.

the silicon surface. A stoichiometric interface was produced by depositing a layer of HfO₂ and then a final layer of HfO, giving a final configuration of Hf₁₆O₃₂. Finally, a fully saturated interface, where there is in principle enough oxygen to saturate all the dangling bonds, was created by adding an additional layer of oxygen atoms on top of the stoichiometric interface, resulting in the configuration Hf₂₄O₄₀.

III. INTERFACE CHARACTERIZATION

A. Physical structure

Initially we consider just the properties of the interfaces as produced via simulated annealing, i.e., without any modification after annealing and relaxation. Figure 2 shows the final nonstoichiometric interface, and we see clearly deep penetration of interface atoms into the silicon surface. This is a result of two competing processes: (i) excess oxygen oxidizes the silicon substrate and forms a SiO_x suboxide layer. Silicon oxidation is strongly exothermic and is controlled by oxygen diffusion into the Si substrate; (ii) the oxygen deficiency during the deposition leaves many unsaturated hafnium electrons, causing hafnium to form Hf-Si bonds. The competition between these two processes results in a rather complex bonding configuration of the annealed structure, characterized by the intermixture of hafnium oxide, hafnium silicide, hafnium silicate, and silicon oxide structural elements, which is quite different from the initial (unrelaxed) structure. In order to analyze the interface structure, it is convenient to divide it into several regions as shown in Fig. 2: region I consists of the bulk Si atoms of the Si substrate; the interface region II contains mostly silicon suboxide referred to as inter-Si and-O (some inter-Si is also in region III); region III to V contain Hf and O atoms bonded to each other. The calculated electron densities of states projected (PDOS) on the atoms in different regions are shown in Fig. 3.

For the bulk silicon we see a small band gap (noting DFT's tendency to underestimate the gap), but this gap is of

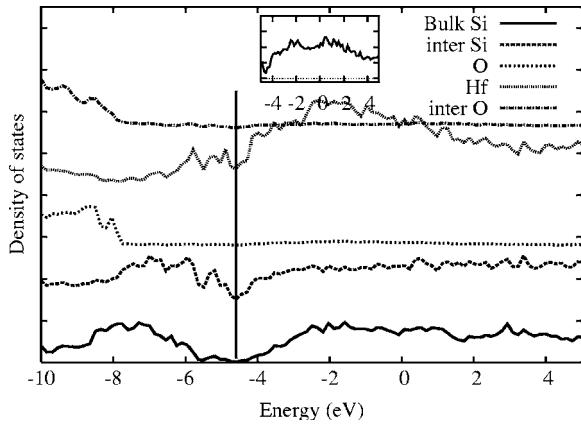


FIG. 3. Projected density of states for the nonstoichiometric Si-HfO₂ interface. Bulk Si corresponds to silicon atoms in region I of Fig. 2, and inter-Si to silicon atoms in regions II and III. The vertical line marks the Fermi energy at the highest occupied molecular orbital. The inset is a blow up of the PDOS of inter-O above the Fermi energy.

critical importance—any states from the interface which lie in this gap will form charge traps in the device. For states of oxygen character, we see clearly a large gap between the valence band and weak conduction band. This demonstrates that all the oxygen is used in forming SiO₂/HfO₂, as indicated by the structure of the interface. In contrast, however, the inter-Si states and Hf states show clearly metallic character, with occupied states at the Fermi energy—there are significant Hf-Si and Hf-Hf bonds across the interface, resulting in no band gap.

Figure 4 shows the final structure for the stoichiometric interface—we see immediately a reduction in the penetration of O and Hf into the interface. In this case Hf does not displace significantly towards the interface, and oxygens only occupy the region between the hafnia layer and the O-terminated silicon surface. The saturation of the hafnium bonds in this stoichiometric structure means that the main structural changes observed during annealing are related to

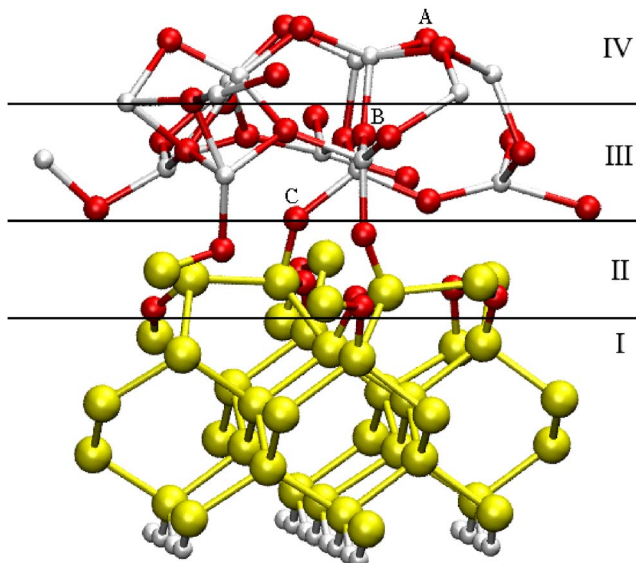


FIG. 4. (Color online) Relaxed structure of the stoichiometric Si-HfO₂ interface. The top, middle and interface oxygen atoms removed to create vacancies are labeled A, B, and C, respectively.

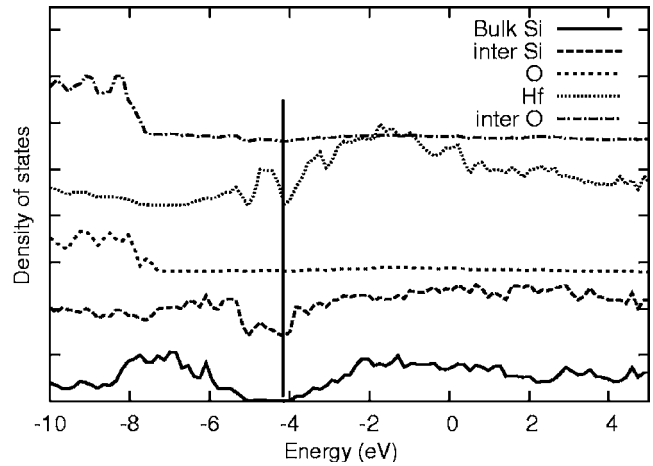


FIG. 5. Projected density of states for the stoichiometric Si-HfO₂ interface. Bulk Si corresponds to silicon atoms in region I of Fig. 2, and inter-Si to silicon atoms in region II.

oxidation of the silicon [process (i) described previously]. Oxygens still penetrate into the upper silicon layer, but interface disruption is much less as they are not competing with Hf. However, if we look at the PDOS of this interface (see Fig. 5) we see that there is a localized state in the band gap which appears just below the Fermi level in the PDOS of Hf and interface Si atoms—this spans the entire bulk Si gap. Despite the apparent separation in the geometry of the interface, this clearly indicates that metallic bonds are still present—if we plot the charge density associated with this defect state (see Fig. 6) we can see that the majority of the state's density lies between neighboring Hf atoms. If we examine the coordination of Hf in the interface, we see that in general Hf is four- and five-coordinated near the interface—well short of the seven-coordination in bulk hafnia.

Noting the presence of these metallic bonds even in the stoichiometric interface, and assuming a constant supply of oxygen from the ambient, we add a saturating layer of oxygen. The resulting structure is shown in Fig. 7. Here we see that regions I and II are almost identical to the original stoichiometric interface, but that the hafniums responsible for

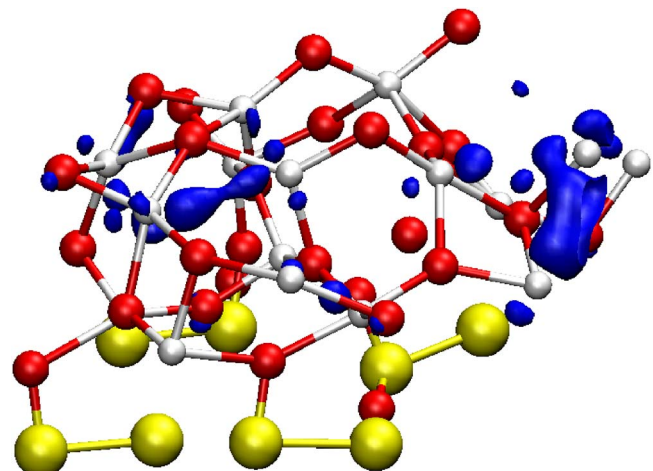


FIG. 6. (Color online) Isosurface of charge density projected onto single particle states associated with defect state seen in Fig. 5 at about -5 eV. Bond density shown is associated with Hf-Hf bonds.

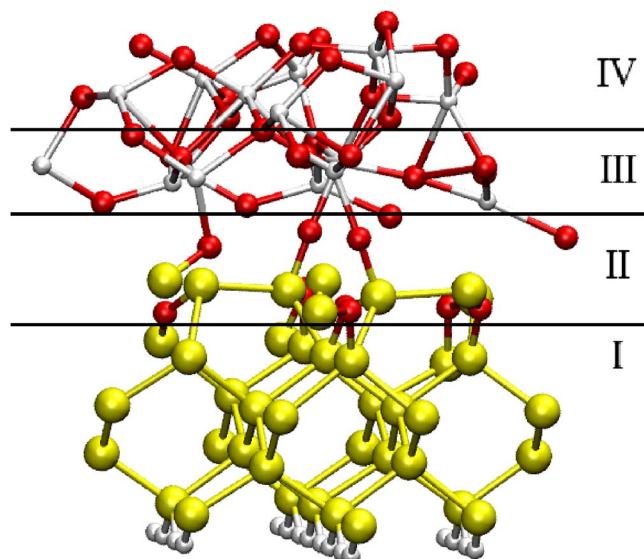


FIG. 7. (Color online) Relaxed structure of the stoichiometric Si-HfO₂ interface after addition of saturating oxygen layer.

the metallic bonds in region III are now saturated. Figure 8 shows the PDOS for the fully saturated structure. As expected we have a clear band gap in the DOS projections, and no longer see any obvious states in the gap. However, we notice that the valence and conduction band edges for silicon and hafnia match almost exactly, giving zero band offset between them. If we look in detail at Fig. 9, we see that the narrow hafnia gap, and hence the small offset with silicon, is due to the presence of states of mainly inter-Si character, and some inter-O and -Hf character at about -6 eV. A plot of the electron density around -6 eV (see Fig. 9) demonstrates the presence of three clear Hf-Si bonds, as well as the expected interface O states. This defect state is characteristic of the oxygen “arm vacancy” reported in previous studies,²⁸ and if we add an oxygen to this site it forms an Hf-O-Si bond, removing one of the Hf-Si bonds.

B. Defected interfaces

In order to understand more clearly the relationship between the bonding environment of the interface and the re-

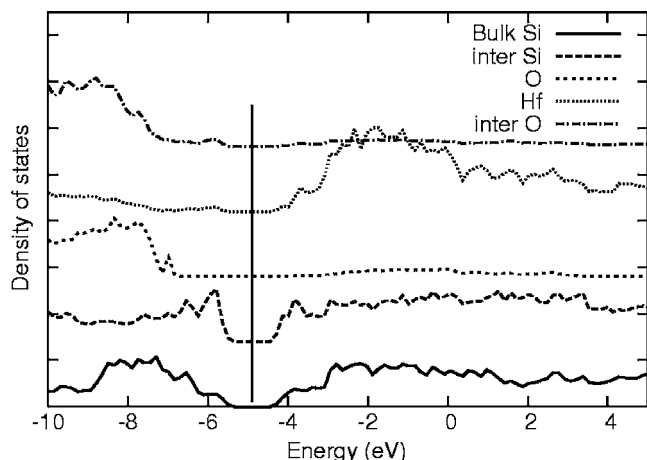


FIG. 8. Projected density of states for the fully saturated Si-HfO₂ interface. Bulk Si corresponds to silicon atoms in region I of Fig. 3, and inter-Si to silicon atoms in region II.

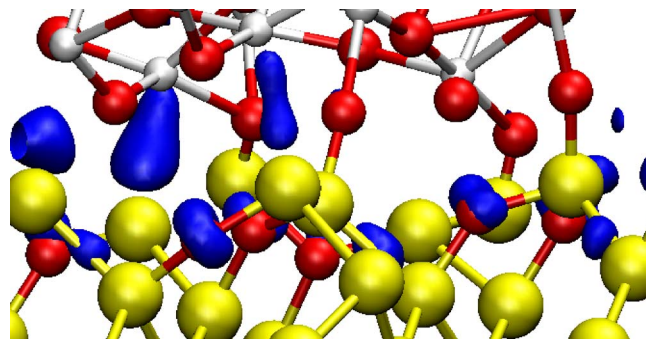


FIG. 9. (Color online) Isosurface of charge density projected onto single particle states associated with defect state seen in Fig. 5 at about -6 eV. Bond density shown is associated with Hf-Si bonds.

sulting electronic structure we also considered neutral oxygen vacancies at different regions of the interface (see A, B, and C in Fig. 4). Site A is a two-coordinated oxygen bonding to two Hf atoms, site B is a three-coordinated oxygen bonded to Hf, and site C is a two-coordinated oxygen between a Si and a Hf. Removal of an oxygen from the top of the interface at site A has the least influence on the electronic structure of the system [see Fig. 10(a)], as expected for a site little involved in the interface bonding. Vacancies at sites B and C, however, introduce many states near to the Fermi energy, reflecting the introduction of several dangling and metallic bonds [see Figs. 10(b) and 10(c)]. It is quite easy to see that additional vacancies will result in an electronic structure very similar to that for the nonstoichiometric interface.

The neutral vacancy formation energies (with reference to half an oxygen molecule) for the top, middle, and interface regions are 4.63, 5.42, and 4.52 eV, respectively—all significantly smaller than the bulk HfO₂ value of 6.48 eV (for three-coordinated oxygen in bulk monoclinic hafnia⁹). The top (A) vacancy has an unusually low formation energy as it is effectively a surface site, but the other two values show that it is much easier to produce a vacancy near to the interface. This agrees with previous studies,²⁸ and indicates that vacancies are likely to migrate towards the interface if present in the bulk oxide.

C. Electron transport

In order to characterize the electrical performance of the considered interfaces, let us discuss their electronic conductance in the ballistic regime.^{24,25} The conductance was calculated by positioning the interface models between two electrodes described by a structureless metal (jellium) model. This method has been shown previously to provide a good model of metal contacts.²⁹ The electrodes are specified by a charge density or equivalently by the radius (r_s) of a sphere containing a unit charge (e). We used $r_s=2$ for the *oxide electrode* and $r_s=3.1$ as the *silicon electrode*. In our tests the tunnelling results were not particularly sensitive to changes in the jellium charge density (assuming we still have metallic leads), but detailed understanding would require a full comparison with atomistic leads. However, in this study we are comparing the interface properties rather than the leads, and it is satisfactory to have a standard set of leads for the all the calculations.

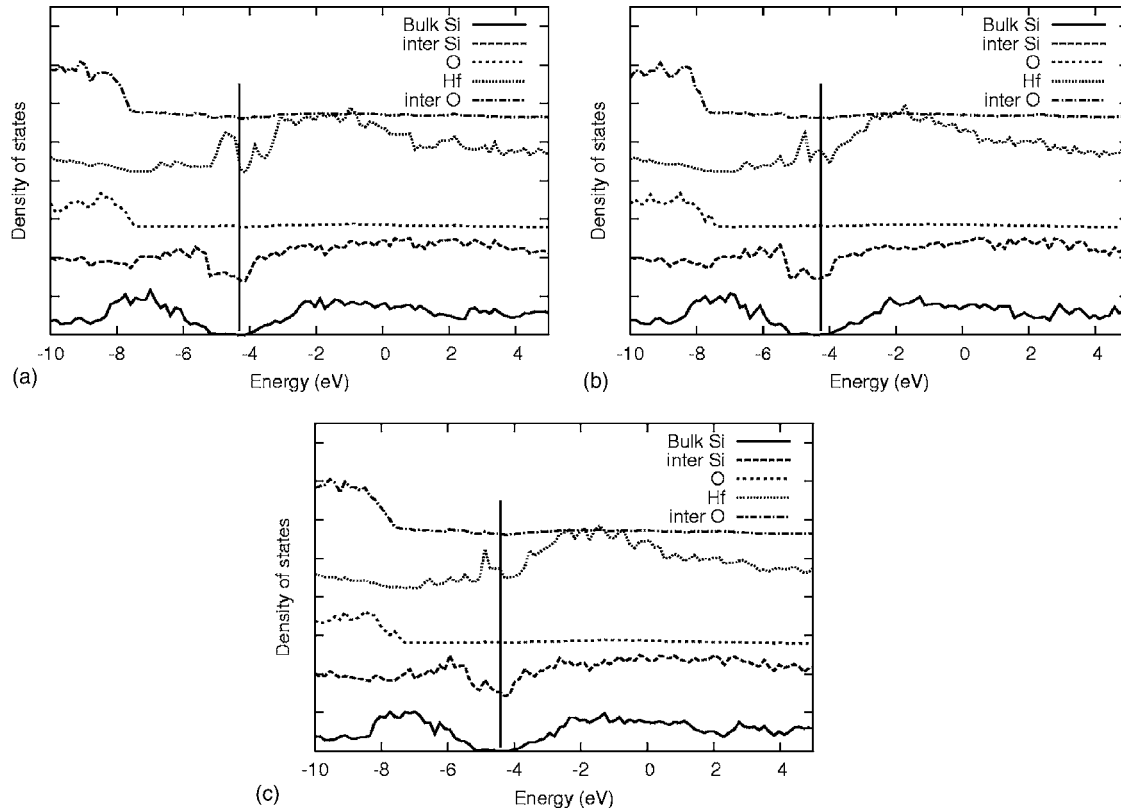


FIG. 10. PDOS for HfO_2 with an oxygen vacancy at positions (a) A, (b) B, and (c) C in Fig. 4.

The conductance of the interfaces can be directly estimated by considering the tunneling probability at the Fermi energy, assuming an infinitesimal bias voltage. The calculated tunneling probabilities as functions of energy are shown in Fig. 11. Here we also include a benchmark model (d) based on the interface used in Ref. 14, but slightly reduced in size to make it computationally manageable²⁸ (Fig. 11). It is seen in Fig. 12 that the interface structures (a) and (b) show clearly metallic behavior, with a large tunneling probability at the Fermi energy. Although in principle the stoichiometric interface (b) has a much lower density of metallic bonds, it is clear that in both cases two channels with roughly unit probability dominate the transport—the localized defect state in the gap of system (b) plays an equivalent role in transport to the fully metallic interface (a). The saturation of dangling bonds in the model (c) results in a reduction of the tunneling probability, but it remains significant at the Fermi energy, again emphasizing the dominance of metallic bonds in the tunneling profile.

Another factor strongly affecting the tunneling probability is the thickness of the dielectric layer. This is seen by comparing interfaces (c) and (d). The latter model is almost twice as thick as the former one. As a result, the tunneling probability at the Fermi level through model (d) is almost an order of magnitude smaller, despite the very similar electronic structure of two models. We can also compare to some degree the transport results for the benchmark interface with those reported previously.¹⁴ Assuming Ohmic behavior we can extrapolate our zero bias conductance to roughly estimate the current density at 1 V. We obtain a value of about 10^7 A/cm², which is several orders of magnitude larger than

the results in Ref. 14 but quite close to the current density when certain defects are present. This significant difference is dominated by the choice of leads in the two works, as we use metallic leads, whereas atomistic bulk silicon leads have been used in Ref. 14.

IV. CONCLUSIONS

Using first principles calculations and simulated annealing we have generated three model hafnia-silicon interfaces. For a nonstoichiometric interface we find that the severe undercoordination of hafnium atoms causes them to diffuse towards the silicon surface. We also see that oxygen tends to penetrate the silicon surface and oxidize Si-Si back bonds. The resulting interface contains several Hf-Si bonds, and is metallic. A stoichiometric interface is much more stable in terms of hafnium atoms penetrating the silicon surface, but we still find that the propensity of silicon to form silicon dioxide leaves dangling hafnium bonds. They can only be saturated by silicons, and localized defect states appear in the silicon band gap. Adding a terminating oxygen layer to this interface saturates most of the metallic bonds, opening a significant band gap with no defect states. However, a few weak Hf-Si bonds remain, reducing the gap width and resulting in zero offset between hafnia and silicon bands. Our electron transport simulations emphasize the influence of even a small number of metallic bonds across the interface, with significant tunneling probabilities observed at the Fermi energy for all the interfaces considered.

In general, despite initially following the bonding rules established in Ref. 15 we find that the static picture of the

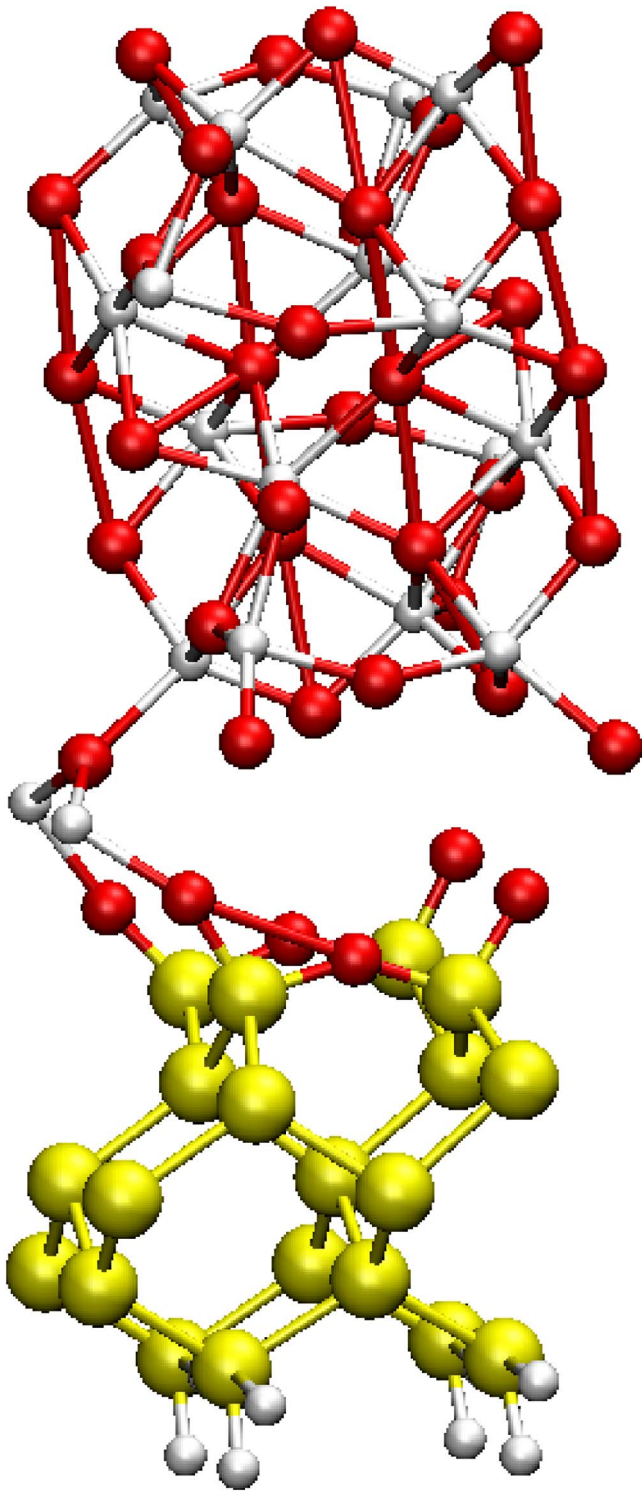


FIG. 11. (Color online) Relaxed structure of the benchmark interface Ref. 28 11. [interface (d) in the text]. Note that oxygen atoms at the right of the interface form further bonds with hafnium atoms in the next periodic cell.

interface is not physical, and at finite temperature, idealistic interface models break down. We find that the propensity of oxygen to diffuse into silicon to form a silicon dioxide layer results in a high probability of dangling Hf bonds being created. If the density of dangling bonds is high enough this results in Hf diffusion towards the interface, but even in for a system with excess oxygen (i.e., the saturated stoichiometric interface) this encourages the generation of some

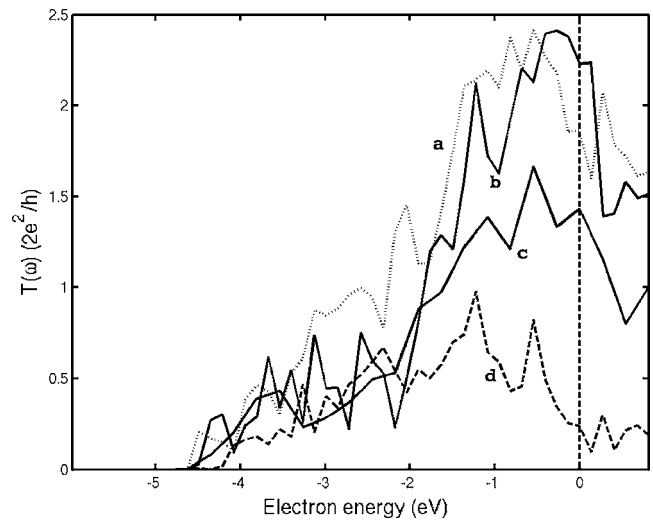


FIG. 12. Tunneling probability through (a) nonstoichiometric interface, (b) stoichiometric interface, (c) saturated interface, and (d) benchmark interface. The oscillations in the tunneling probabilities are an artifact of the calculation sampling density.

weak Hf–Si bonds. These metallic bonds significantly reduce the effective band gap at the interface and the band offset with silicon, and are a dominant channel for electron transport.

If we compare our simulated *growth* method to experiments, it is clear that the direct deposition of O and Hf species onto the surface is most comparable to pulsed laser deposition^{30,31} and remote plasma oxidation.^{32–34} In these techniques either Hf or Hf and O directly reacts with the surface, and the resulting interface depends strongly on the nature of the surface and the ambient oxygen pressure. As our calculations predict, these experiments demonstrate the particular sensitivity of silicide formation (Hf–Si bonds) on the stoichiometry of the oxide and oxygen pressure.³¹ Furthermore, they show that deposition of severely undercoordinated Hf on a fully formed silicon oxide layer results in diffusion of oxygen out of silica in an attempt to form a stoichiometric hafnia layer. Our results suggest that this process cannot be sustained, and without an external source of oxygen, silicide formation will result.

The obvious implication of this discussion is that the interface structure must be stabilized to prevent diffusion of hafnium and oxygen. Two possibilities immediately suggest themselves: (i) if the SiO₂ layer on the silicon surface is already fully formed and a significant ambient oxygen pressure exist (free oxygen interstitials are highly mobile in monoclinic hafnia, and hence can easily diffuse to heal the interface³⁵), lattice oxygen atoms will have less incentive to diffuse to the interface. Despite the reduction in effective dielectric constant, the benefits of a stable interface may make this a more effective design; (ii) the interface could be stabilized externally, e.g., if dangling hafnium bonds are saturated by some other species during growth, it may prevent metallization. Simulations²⁸ suggest that in atomic layer deposition (and by implication, also chemical vapor deposition), the chemical precursors stabilize the interface by saturating dangling bonds, allowing a *cleaner* structure to form. Both these directions are the topics of future studies.

ACKNOWLEDGMENTS

The authors acknowledge the generous computer resources from the Center for Scientific Computing, Espoo, Finland. This research has been supported by the Academy of Finland through its Centers of Excellence Program (2000-2005). One of the authors (J.L.G.) acknowledges funding by SEMATECH.

- ¹A. I. Kingon, J. P. Maria, and S. K. Streiffer, *Nature* (London) **406**, 1032 (2000).
- ²*High k Gate Dielectrics*, edited by M. Houssa (IOP, London, 2003).
- ³A. M. Stoneham, J. L. Gavartin, and A. L. Shluger, *J. Phys.: Condens. Matter* **17**, S2027 (2005).
- ⁴H. R. Huff *et al.*, *Microelectron. Eng.* **69**, 152 (2003)
- ⁵G. D. Wilk, R. M. Wallace, and J. M. Anthony, *J. Appl. Phys.* **89**, 5243 (2001).
- ⁶C. D. Young, G. Bersuker, G. A. Brown, P. Lysaght, P. Zeitzoff, R. W. Murto, and H. R. Huff, in *IEEE International Reliability Physics Symposium* (IEEE, New York, 2004), p. 597.
- ⁷G. Bersuker, P. Zeitzoff, G. Brown, and H. R. Huff, *Mater. Today* **2**, 26 (2004).
- ⁸V. V. Afanas'ev and A. Stesmans, *J. Appl. Phys.* **95**, 2518 (2004).
- ⁹A. S. Foster, F. L. Gejo, A. L. Shluger, and R. M. Nieminen, *Phys. Rev. B* **65**, 174117 (2002a).
- ¹⁰R. Choi, S. C. Song, C. D. Young, G. Bersuker, and B. H. Lee, *Appl. Phys. Lett.* **87**, 122901 (2005).
- ¹¹M. Houssa, S. D. Gendt, J. L. Autran, G. Groeseneken, and M. M. Heyns, *Appl. Phys. Lett.* **85**, 2101 (2004).
- ¹²J. L. Gavartin, A. S. Foster, G. I. Bersuker, A. L. Shluger, and R. M. Nieminen, *J. Appl. Phys.* **97**, 053704 (2005).
- ¹³V. Fiorentini and G. Gullery, *Phys. Rev. Lett.* **89**, 266101 (2002).
- ¹⁴L. R. C. Fonseca, A. A. Demkov, and A. Knizhnik, *Phys. Status Solidi B* **239**, 48 (2003).
- ¹⁵P. W. Peacock and J. Robertson, *Phys. Rev. Lett.* **92**, 057601 (2004).
- ¹⁶R. Puthenkovilakam and J. P. Chang, *J. Appl. Phys.* **96**, 2701 (2004).
- ¹⁷B. J. O'Sullivan *et al.*, *J. Electrochem. Soc.* **151**, G493 (2004).
- ¹⁸M. Copel, M. C. Reuter, and P. Jamison, *Appl. Phys. Lett.* **85**, 458 (2004).
- ¹⁹J. Junquera, O. Paz, D. Sánchez-Portal, and E. Artacho, *Phys. Rev. B* **64**, 235111 (2001).
- ²⁰J. M. Soler, E. Artacho, J. D. Gale, A. García, J. Junquera, P. Ordejón, and D. Sánchez-Portal, *J. Phys.: Condens. Matter* **14**, 2745 (2002).
- ²¹J. P. Perdew, K. Burke, and M. Ernzerhof, *Phys. Rev. Lett.* **77**, 3865 (1996).
- ²²A. A. Demkov, L. R. C. Fonseca, E. Verret, J. Tomfohr, and O. F. Sankey, *Phys. Rev. B* **71**, 195306 (2005).
- ²³Y. Xue, S. Patta, and M. A. Ratner, *Chem. Phys.* **281**, 151 (2002).
- ²⁴P. Havu, V. Havu, M. J. Puska, and R. M. Nieminen, *Phys. Rev. B* **69**, 115325 (2004).
- ²⁵P. Havu, V. Havu, M. J. Puska, M. H. Hakala, A. S. Foster, and R. M. Nieminen, *J. Chem. Phys.* **124**, 054707 (2006).
- ²⁶A. Nitzan, *Annu. Rev. Phys. Chem.* **52**, 681 (2001).
- ²⁷C. J. Först, C. R. Ashman, K. Schwarz, and P. E. Blöchl, *Nature* (London) **427**, 53 (2004).
- ²⁸J. L. Gavartin, L. Fonseca, G. Bersuker, and A. L. Shluger, *Microelectron. Eng.* **80**, 412 (2005).
- ²⁹J. Bormet, J. Neugebauer, and M. Scheffler, *Phys. Rev. B* **49**, 17242 (1994).
- ³⁰S. J. Wang *et al.*, *Appl. Phys. Lett.* **82**, 2047 (2003).
- ³¹D. Y. Cho, K.-S. Park, B.-H. Choi, S.-J. Oh, Y. J. Chang, D. H. Kim, T. W. Noh, and S. D. Bu, *Appl. Phys. Lett.* **86**, 041913 (2004).
- ³²B. H. Lee, L. Kang, R. Nieh, W.-J. Qi, and J. C. Lee, *Appl. Phys. Lett.* **76**, 1926 (2000).
- ³³K. Yamamoto, S. Hayashi, M. Niwa, M. Asai, S. Horii, and H. Miya, *Appl. Phys. Lett.* **83**, 2229 (2003).
- ³⁴H. Takeuchi, D. Ha, and T.-J. King, *J. Vac. Sci. Technol. A* **22**, 1337 (2004).
- ³⁵A. S. Foster, A. L. Shluger, and R. M. Nieminen, *Phys. Rev. Lett.* **89**, 225901 (2002).